ISSN 1814-4225 (print)
ISSN 2663-2012 (online)

UDC 621.383.52:546.28 **doi: 10.32620/reks.2023.1.07**

Mykola KUKURUDZIAK[1, 2]

[1] ***Rhythm Optoelectronics Shareholding Company, Chernivtsi, Ukraine***
[2] ***Yu. Fedkovych Chernivtsi National University, Chernivtsi, Ukraine***

SILICON FOUR ELEMENT p-i-n PHOTODIODE WITH IMPROVED CHARACTERISTICS

This article presents the results of the development of silicon coordinate p-i-n photodiodes (PD) with improved parameters. The technological possibilities of reducing the gaps between the responsive areas of multi-element PDs were studied. PDs with reduced gaps were modeled, samples were made according to the models, the parameters of the obtained PDs and the influence of various technological factors on their values were investigated. During research, it was established that the factor that limits the possibility of reducing the gaps is the insulation resistance between the responsive elements. The decrease in the insulation resistance between the PD elements was a consequence of the formation of inversion leakage channels at the Si-SiO2 interface, which is characteristic of high-resistance p-type silicon, the conductivity of which increased with a decrease in the width of the gaps. To increase the resistance of the gaps between the platforms and reduce the influence of inversion layers, it was decided to form regions of the restriction of the leakage channels between the REs – highly doped regions isotypic with the substrate material (p^+-type). They will prevent the movement of current carriers that are generated in the inversion layers on the surface of the substrate. Four-element p-i-n photodiodes with 31 μm gaps between the sites were made. The proposed PD is not significantly inferior in parameters to analogues, but it is the sample with the smallest gaps between RE among photodiodes of the same type and size in the world market. The improvement of the insulation resistance between the REs made it possible to reduce the level of dark current of the PD by twice compared to serial products, with a slight decrease in responsivity due to the introduction of additional thermal operations into the technological route. In particular, the dark current density of the RE of experimental PDs was 40-80 nA/cm^2, compared to 80-250 nA/cm^2 for commercial samples. Impulse current monochromatic sensitivity at a wavelength of 1064 nm for experimental samples was 0.41-0.44 A/W, and for commercial ones - 0.45-0.48 A/W.

Keywords: *photodiode; responsive elements; responsivity; dark current; insulation resistance.*

Introduction

Photoreceptors (PR) are one of the main components of optoelectronic devices and systems. The needs of optoelectronics stimulate the creation of PRs with high speed, responsivity, minimal noise, and the ability to work in different ranges of wavelengths, etc. An urgent task of modern optoelectronics and photoelectronics is the development of systems for detecting the coordinates of various objects. Coordinate multi-element [1] or matrix [2] p-i-n photodiodes (PD) are most often used in such systems. Semiconductor photodetectors, the output signal of which is determined not only by the intensity and spectral composition of the radiation, but also by the coordinates of the irradiated area on the responsive elements (RE), are called coordinate PD. The coordinate PD is usually a two- or four-element (sometimes more) photodiode on one semiconductor plate, and the REs are separated by gaps smaller than the size of the light probe.

Formulation of the task

To increase the accuracy of determining the coordinates of objects, it is necessary to reduce the gaps between the REs (d), this is also relevant when reducing the diameter of the light probe. Thus, in ophthalmic equipment, the PR must have a resolution sufficient to transmit small details of the fundus and a high signal-to-noise ratio to reproduce the image of the fundus with the necessary contrast [3, 4]. A laser beam is also used to detect cantilever deflection in atomic force microscopy. It is directed to the back side of the cantilever, which is covered with a special aluminum mirror layer for the best reflection, and the reflected beam enters a special four-element PD. Thus, deviations of the cantilever lead to a shift of the laser beam relative to the sections of the photodiode, accordingly, a change in the difference signal from the PD will show the amplitude of the shift of the cantilever in one direction or another [5]. Here, it is also worth using PRs, which will ensure the most accurate determination of the coordinates of the cantilever placement. Additionally, multielement PDs are used to determine the coordinates of objects in space based on the reflected beam, in particular, to register targets in the homing heads of anti-tank missile systems.

Accordingly, the need to develop and manufacture highly responsive multi-element PRs, in particular PDs with reduced gaps between REs to increase the resolving power of optoelectronic systems and increase the

accuracy of determining the coordinates of objects is an urgent scientific and technical task.

Analysis of the latest research and industrial samples

Leading PRs productions are engaged in the development and serial production of coordinate PDs. Thus, PD 342M (Orion Shareholding Company, RF) [6], PD YAG-555-4 (Excelitas Technologies Corp., Taiwan) [7] and PD-15M-01 (Rhythm Optoelectronics Shareholding Company, Ukraine) [8] have gaps between REs 200 μm, PD QP154-Q (First Sensor AG, Germany) – 70 μm [9]. It should be noted that radial-sector PDs with a diameter of 14 mm are given for operation at a wavelength of λ = 1.064 μm. Also, [10] presents the results of work on improving the parameters of silicon quadrant photodiodes with a gap between the REs of 50 μm and the diameter of the RE of 3 mm. Scientists are also actively engaged in the improvement of object registration systems, and not only their components. In particular, [11] provides a model and algorithm for training a small object detection system for small unmanned aerial vehicles.

Formulation of the purposes of the article

Considering the needs of the world market, the purpose of this work is to study the technological possibilities of reducing the gaps between REs and manufacturing PDs with the minimum value of this parameter. Note that the samples of the leading PRs manufacturers have pulsed current monochromatic responsivity $S_{pulse} > 0.4$ A/W [8, 9] and current responsivity on the modulated flow $S_{I\lambda} > 0.4$ A/W [7] with a value of the dark current (I_d) of the order of tens nano amperes. Accordingly, the obtained PDs should have no less responsivity than indicated above at low levels of dark currents of REs.

1. Methodology of the experiment

Research was carried out in the manufacture of silicon four-element p-i-n PDs with a guard ring (GR) (Fig. 1) by diffusion-planar technology using the technological modes given in [1]. Diffusion and oxidation processes were carried out in a SDO 125/3-15 furnace. The technological process of manufacturing the lD crystal consisted of various combinations of thermal operations and photolithography: semiconductor substrates were oxidized; photolithography was carried out to create windows for phosphorus diffusion; diffusion of phosphorus to the front side to create n^+-type RE and GR; diffusion of boron to the reverse side of the substrate to create a p^+-type ohmic contact; photolithography for creating contact windows; sputtering of Cr-Au on the front and back sides.

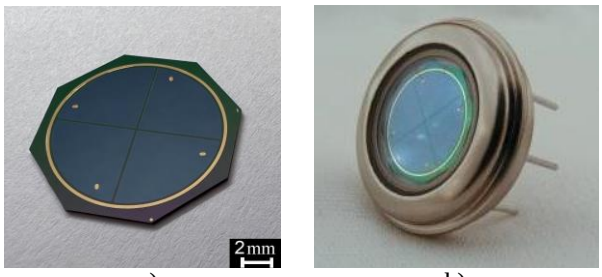

a) b)

Fig. 1. Photo of the crystal (a) and the final photodiode (b)

Dark currents were measured according to the "Method of measuring the dark, total current and photocurrent of photovoltaic semiconductor radiation receivers (PSRR)" [12] using power supplies B5-47 and B5-10, voltmeter V7-23, and probe installation Probe A-5. Determination of the capacity of the REs (C_{RE}) was carried out according to the "Method of measuring the capacity of the PSRR" [12]. The current pulsed monochromatic responsivity was measured at a wavelength of λ = 1.064 μm with a pulse duration τ_i = 500 ns and a load resistance R_l = 10 kΩ according to the appropriate method given in [12]. The measurement of the current monochromatic static responsivity on the modulated flow was carried out at λ = 1.064 μm and the modulation frequency f = 20 kHz according to the appropriate method [12]. A B5-8 power supply unit, a G5-48 pulse generator, and a C1-99 oscilloscope were used for responsivity measurements. The reverse bias voltage was U_{bias} = 120 V.

Determination of the insulation resistance between REs ($R_{RE\text{-}RE}$) was carried out according to the equivalent electrical circuit shown in Fig. 2.

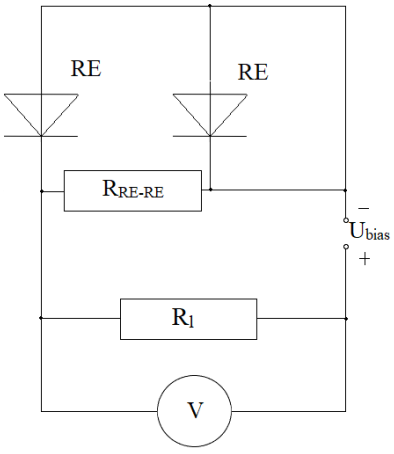

Fig. 2. Equivalent electrical scheme of $U_{RE\text{-}RE}$ measurement

ISSN 1814-4225 (print)
ISSN 2663-2012 (online)

The voltage between the REs ($U_{RE\text{-}RE}$) was measured at U_{bias}=2 V and the load resistance R_l=10 kΩ, after which $R_{RE\text{-}RE}$ was calculated according to formula (1):

$$R_{RE-RE} = \frac{(U_{bias}-U_{RE-RE})R_l}{U_{RE-RE}}. \quad (1)$$

2. Experimental

To assess the possibility of manufacturing PD with reduced gaps using the technology described above, samples were made using the same technological route with gaps between REs 200 (Fig. 3, a), 130, 70, 50 (Fig. 3, b), 30 (Fig. 3, c) μm. The main controlling parameter in the preparation of samples was $R_{RE\text{-}RE}$. This parameter should reach the highest possible values to prevent the flow of charge carriers from one RE to another both at room temperature and during operation at elevated temperatures, as well as to minimize the photocoupling coefficient.

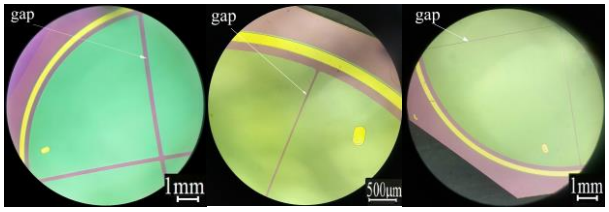

a) b) c)

Fig. 3. Images of photodiode surface areas with different by the values of the gaps between the REs: a) d=200 μm; b) d=50 μm; c) d=30 μm

When the value of d decreases, a decrease in the $R_{RE\text{-}RE}$ is observed, which can be seen from Table 1.

Table 1

$R_{RE\text{-}RE}$ values at different values of the gaps between the REs

d, μm	200	130	70	50	30
$R_{RE\text{-}RE}$, Ω	13.3-14.3·10⁶	5.7-9.5·10⁶	2.5-4.4·10⁶	76.8-156.7·10³	0.1-1.7·10³

At d=50 μm, the electrical resistance between the REs reached a critical value – in fact, the 4-element PD functioned as a single-element one, since all the REs were short-circuited, such a sample had a photocoupling factor of the order of 80-90 %. The decrease in the insulation resistance between the PD elements was a consequence of the formation of inversion leakage channels at the Si-SiO_2 interface, which is characteristic of high-resistance p-type silicon [13, 14]. The conductivity of these channels increased with a decrease in the width of the gaps. Accordingly, according to this technological route, the production of suitable samples with d ≤ 50 μm is impossible.

To increase the resistance of the gaps between the REs and reduce the influence of inversion layers, it was decided to form leakage channel restriction regions between the REs - highly doped regions isotypic with the substrate material (p^+-type) [15]. They will prevent the movement of current carriers that are generated in the inversion layers on the surface of the substrate. To reduce the influence of the crystal periphery on the dark currents of the GR, as well as to increase the insulation resistance between the GR and the REs, it was decided to form p^+-layers on the periphery of the crystal and in the gaps between the GR and the REs. This was implemented by introducing two additional thermal operations (boron diffusion and oxidation) and one photolithography into the technological route. After changing the route, the sequence of PD crystal manufacturing operations is shown in Fig. 4.

When manufacturing PDs according to the described route and reducing the gaps between the REs, it is necessary to take into account the sizes of the regions of the output of the n^+-p- and p^+-p-junctions to the surface of the plate and to form the boundary conditions for the production of photo templates with minimal gaps.

3. Discussion of research

One of the main tasks in the manufacture of PD with reduced gaps is to ensure the proper insulation resistance of the REs between themselves, which decreases as a result of the appearance of inversion channels. We note that the research and production of PD was carried out on the basis of p-Si with a specific resistance ρ=16-18 kΩ·cm. According to [15], inversion layers on the p-type silicon surface are already present at ρ=1-10 Ω·cm. The general reasons for the appearance of inversion layers have long been known and studied [13]. The key factor in their formation is an increase in the specific resistance of the base material, since with an increase in ρ of the material, a smaller amount of impurities is needed to change the surface conductivity to the opposite [16]. The technological reasons for the appearance of inversion are improper chemical treatment of substrates, the presence of alkali metal impurities in deionized water, quartz vessels, or a quartz reactor, and carrier gases. Inversion can also be caused by the diffusion and redistribution of impurities in SiO_2 introduced during previous thermal operations to the Si-SiO_2 interface [17]. Precise control of the specified factors and a decrease in the specific resistance of silicon can make it possible to manufacture a PD with reduced gaps between the REs without the introduction of p^+-layers due to the minimization of the appearance of inversion layers. But with a decrease in the ρ of the material (and, accordingly, the life time of non-basic

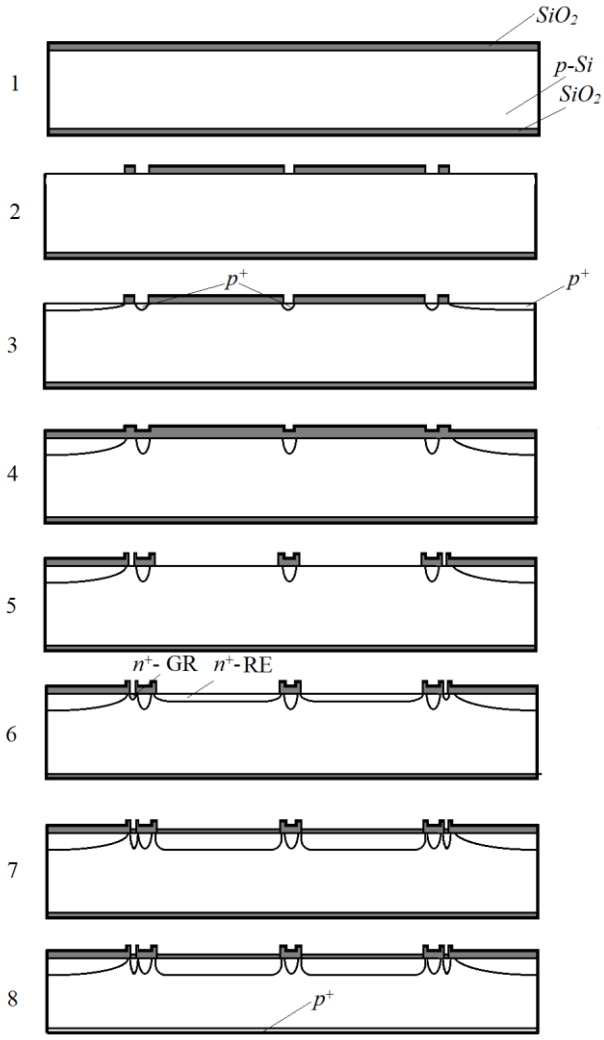

Fig. 4. Schematic section of a PD crystal at various stages of production: 1) oxidation of silicon substrates; 2) photolithography for the formation of windows for boron diffusion; 3) diffusion of boron to the front side of the crystal; 4) oxidation / boron drive-in – to mask the p^+-layer and increase the depth of the p^+-p-junction; 5) photolithography for the formation of windows for phosphorus diffusion; 6) diffusion/predeposition of phosphorus; 7) phosphorus drive in - to increase the depth of the n^+-p-junction and the formation of anti-reflective SiO_2; 8) diffusion of boron to the rear side of the substrate to create an ohmic p^+-layer and heterization of generation-recombination centers

charge carriers τ), the responsivity will decrease and the capacity of the RE will increase [1]:

$$S = e\beta\alpha(\tau_n\mu_n + \tau_p\mu_p), \quad (2)$$

where e is the charge of the electron;

β is the quantum yield;

α is absorption coefficient;

τ_n, τ_p are lifetime of electrons and holes, respectively;

μ_n, μ_p are mobility of electrons and holes, respectively.

$$C_{RE} = A_{RE}\left(\frac{\varepsilon\varepsilon_0 eN_A}{2(\phi_k - U_{bias})}\right)^{\frac{1}{2}}, \quad (3)$$

where A_{RE} is effective area of RE;

ε, ε_0 are dielectric constants for silicon and vacuum, respectively;

φ_k is contact potential difference;

N_A is impurity concentration in the substrate.

Note that the dark current, in particular its generation-recombination component (I_G), is inversely proportional to the lifetime of non-basic charge carriers [18]:

$$I_G = e\frac{n_i}{2\tau}W_i A_{RE}, \quad (4)$$

where n_i is own concentration of charge carriers in the substrate;

W_i – space charge region width.

4. Calculations

4.1. Estimation of the size of the output regions of n^+-p- and p^+-p-junctions on the plate surface

When determining the dimensions of the output regions of n^+-p- and p^+-p-transitions on the surface of the plate, it is necessary to take into account the lateral diffusion under the masking oxide [16], the width of which can be determined from the equation [17]:

$$l_{lat} \approx 0.8x_j, \quad (5)$$

where l_{lat} – lateral diffusion width;

x_j – p-n junction depth.

To estimate l_{lat}, it is necessary to determine the final x_j. The diffusion of phosphorus and boron was carried out by two-stage diffusion in both cases. First, we carried out predeposition – short diffusion from a source of infinite power at temperature T_1, obtaining a thin diffusion layer in the substrate. After that, drive-in was carried out at a higher temperature T_2 so that $D_2T_2 >> D_1T_1$ (D – diffusion coefficients), while the thin diffusion layer was a source with a limited amount of impurity. Note that after the operations of boron and phosphorus diffusion to the front side of the substrate, other thermal operations are carried out that increase x_j. Taking into account that in our case, some difficulties arise during calculations, because when impurities are introduced into already doped silicon, the values of the diffusion coefficients deviate from the constant value that corresponds to the temperature of the processes, the value

ISSN 1814-4225 (print)
ISSN 2663-2012 (online)

of x_j was obtained experimentally. The depth of n^+-p- and p^+-p-junctions was determined by the spherical grinding method [21]. Accordingly, $x_{n+-p} \approx 4.5$ μm, $x_{p+-p} \approx 5$ μm. The lateral diffusion width will be $l_{lat}^{p+} \approx 4$ μm and $l_{lat}^{n+} \approx 3.5$ μm for boron and phosphorus diffusion, respectively.

To avoid overlap of n^+- and p^+- regions due to lateral diffusion on the surface of the plate, it is worth introducing a correction Δ_1, which will characterize the distance between these regions. For technological reasons, $\Delta_1 = 2$ μm.

4.2. Corrections for photolithography

When performing photolithography for the formation of small elements, in this case gaps between RE, it is worth considering some factors that affect the accuracy of the process. In particular, the etching of the masking oxide is usually accompanied by lateral etching under the mask [22]. In reality, the speed of lateral etching is lower than in depth, since under the edge of the mask the diffusion processes of the exchange of reaction products and fresh etchant with a lower speed. Correspondingly, the depth of the lateral etching was less than the thickness of the etched layer. However, shallow drawing elements require longer etching time if the process is carried out in a stationary herbarium. Accordingly, with a masking SiO_2 thickness of 0.7-0.8 μm, a correction for lateral etching $\Delta_2 \approx 1$ μm can be introduced.

Another factor to consider during photolithography is the etch wedge at the oxide boundary, which affects the size of the diffusion region. If the walls of the oxide-etched windows were vertical, the size of the diffusion region would differ from the size of the window by the amount of lateral diffusion. In the presence of a wedge, there is an additional increase in the size of the diffusion region, since the thickness of the oxide near the lower edge of the wedge is not sufficient for masking from the diffusing impurity.

The increase in the diffusion area can be estimated using the formula [23]:

$$l_{diff} = l_{SiO2} + 2x_j\left(1 + \frac{k}{10h_{SiO2}}\right), \quad (6)$$

where l_{SiO2} and l_{diff} – the size of the oxide window and the corresponding diffusion region;

k – width of the etching wedge;

h_{SiO2} – thickness of the oxide film.

Considering (5), equation (6) will take the form (7), since in (6) it is assumed that the lateral diffusion width reaches x_j

$$l_{diff} = l_{SiO2} + 1{,}6x_j\left(1 + \frac{k}{10h_{SiO2}}\right). \quad (7)$$

Accordingly, the correction that takes into account the reduction of the width of the gap between the REs due to the etching wedge Δ_3 will be determined from equation (8):

$$\Delta_3 = 1.6x_j\left(\frac{k}{10h_{SiO2}}\right). \quad (8)$$

Note that when using photoresist AZ1518 (MicroChemicals) $k \approx 0.1$ μm. Accordingly, Δ_3 at $h_{SiO2} = 0.7$-0.8 μm reaches about 10 nm.

Note that the photo templates for the diffusion of boron into the front side of the substrate are "inverted" to the photo templates for the diffusion of phosphorus, taking into account the width of the diffusion regions for boron.

Considering the above corrections, the minimum width of the gap between REs (d_{min}), which is possible at a given level of technology, can be determined from equation (9):

$$d_{min} = 2l_{lat}^{n+} + l_B + 2l_{lat}^{p+} + 2\Delta_1 + 2\Delta_2 + 2\Delta_3, \quad (9)$$

where l_B is the width of the boron diffusion region between the REs.

For technological reasons, $l_B = 10$ μm, respectively, $d_{min} \approx 31$ μm. The photo of the gaps between the REs of the proposed PD is shown in Fig. 5.

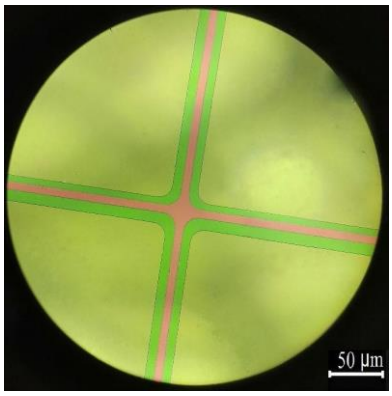

Fig. 5. Photo of gaps between REs with p^+-layer

Note that the distance between the REs and GR was 200 μm, and the width of the p^+-region was 100 μm, so in this case it is not necessary to consider the above corrections.

5. Research results

A silicon quadrant p-i-n PD with GR and gaps between the REs of 31 μm (PD-E) was manufactured. Experimental samples were compared with commercial products PD-15M-01 with d = 200 μm (PD-C), manufactured in a single technological cycle with PD-E. Thus, to evaluate the responsivity in the near-IR range of

wavelengths, the spectral characteristics of the responsivity of experimental and commercial PDs were obtained (Fig. 6).

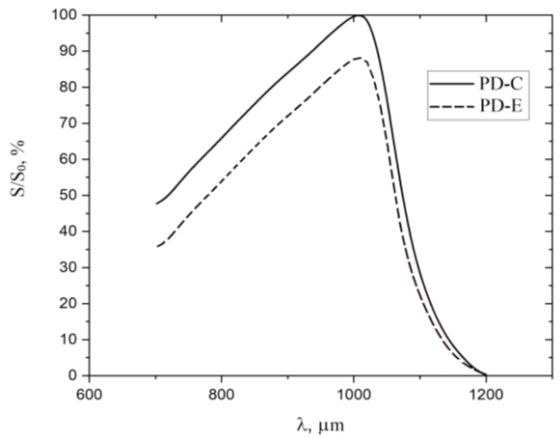

Fig. 6. Spectral characteristics of the responsivity of PD-C and PD-E

From fig. 6, it can be seen that the responsivity of PD-E is 10-12% lower than that of PD-C. This is caused by the introduction of two additional thermal operations into the technological route. Simultaneously, the number of generation-recombination centers (GRCs) increases in the volume and on the surface of the crystal due to the introduction of uncontrolled impurities and the additional formation of point defects due to re-oxidation. The effective lifetime of charge carriers (τ_{eff}) based on the presence of impurities and defects can be determined from equation [18]:

$$\tau_{eff} = \frac{\exp\left(\frac{E_D - E_i}{kT}\right)}{\sigma_{ss-n} N_D v_n} + \frac{\exp\left(\frac{E_i - E_D}{kT}\right)}{\sigma_{ss-p} N_D v_p}, \quad (10)$$

where σ_{ss-n}, σ_{ss-p} – are the capture cross sections for electrons and holes, respectively;

E_D is the energy level of the GRC;

E_i is the energy level corresponding to the middle of the band gap;

k is Boltzmann table;

T is temperature;

N_D is the GRCs concentration;

v_n, v_p are the average relative (relative to the recombination center) velocity of the thermal motion of electrons and holes, respectively.

Accordingly, an increase in the number of GRCs reduces the lifetime of minor charge carriers and responsivity. Thus, at $\lambda = 1.064$ μm for PD-C $S_{pulse} = 0.45$-0.48 A/W, and for PD-E $S_{pulse} = 0.41$-0.44 A/W.

I-V characteristics were also obtained for experimental and commercial samples during reverse displacement (Fig. 7). From fig. 7 it can be seen that I_d in PD-C is twice as high as in PD-E. This is caused by a significant decrease in leakage currents due to the formation of p^+-type regions between the REs and GR. Because of the formation of inversion channels at the interface of Si-SiO_2, it is possible to increase I_d and I_{GR}. As we know from equation (10) that the generation-recombination component of the dark current increases due to the decrease in τ, but as experiments show, this increase is not significant compared to the decrease due to the absence of inversion channels. Note that $R_{RE\text{-}RE}$ in PD-E reached 20-30 MΩ.

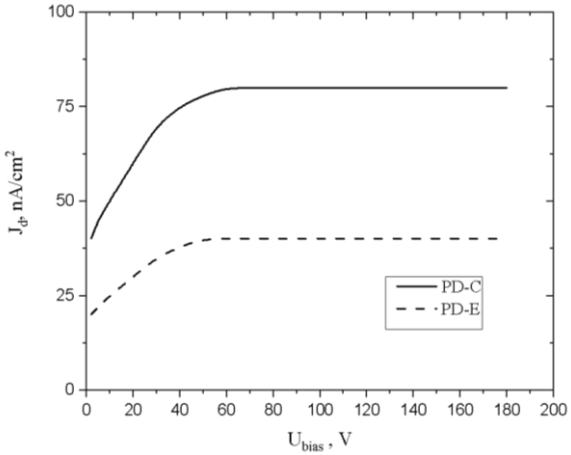

Fig. 7. Typical I-V characteristics for PD-C and PD-E

A graph of the dependence of the RE capacity on the bias voltage was obtained (Fig. 8). The capacity of PD-E does not differ from the capacity of PD-C. Note that the effective area of the RE in PD-E is 5 % larger than the A_{RE} of PD-C, but this difference does not significantly affect the capacity value.

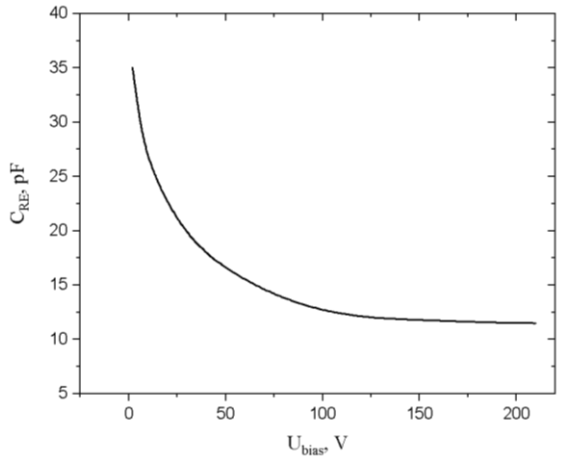

Fig. 8. Dependence of the RE capacity on the bias voltage of PD-E and PD-C (the curves coincide)

To compare the main parameters of PD-E with the parameters of analogs presented on the market, Table 2 was obtained.

ISSN 1814-4225 (print)
ISSN 2663-2012 (online)

Table 2

Parameters of the proposed PD-E in comparison with analogues

Parameter	The value of the parameter				
	Proposed PD-E	**PD-342M «Orion», RF [6]**	**PD-15M-01 «Rythm», Ukraine [8]**	**YAG-555-4 Excelitas Technologies Corp., Taiwan [7]**	**QP154-Q First Sensor AG, Germany [9]**
	Typ / max	Typ / max	Typ / max	Typ / max	Typ / max
Dark current density of the RE, J_d, nA/cm^2	40 / 80	≤ 18000	80 / 250	130 / 385	2.5 / 80
Responsivity on the modulated flow at λ =1.064 μm, $S_{I\lambda}$, A/W	0.44 / 0.48	0.2 ≥	0.46 / 0.5	0.44	-
Pulse responsivity at λ =1.064 μm, S_{pulse}, A/W	0.41 / 0.44	-	0.45 / 0.48	-	0.45 / 0.65
Capacity of RE, C_{RE}, pF	12 / 14	≤ 20	12 / 14	12 / 20	12 / 20
The gap between REs, d, μm	31	200	200	200	70
Bias voltage, U_{bias}, V	120	120	120	180	150

Note. The absence of some parameters in the table is caused by their absence in the technical documentation of the PD.

As can be seen from Table 2, the proposed PD-E is not significantly inferior in terms of parameters to analogues, but it is the sample with the smallest gaps between the REs among photodiodes of the same type and size on the market.

Conclusions

To increase the accuracy of determining the coordinates of objects with the help of coordinate p-i-n photodiodes, photodetectors with gaps between REs of 31 μm were made, which is the best sample among those offered in the market of the same type. The following conclusions were made during the research:

1. When the gaps between the REs are reduced, the insulation resistance between them increases due to the presence of inversion layers at the Si-SiO_2 interface

2. The formation of surface regions of restriction of leakage channels isotypic to the material of the substrate between the REs helps increasing their insulation resistance and allows reducing the width of the gaps. This is embodied by the additional diffusion of boron into the gaps between the REs.

3. The formation of p^+-regions between the REs and between the GR and the REs allows reducing the value of the dark current density of PDs to 40-80 nA/cm^2 compared to 80-250 nA/cm^2 (for commercial samples) with a slight decrease in PD responsivity.

Directions for future research

The proposed structure of the PD crystal can be implemented only by introducing two additional thermal operations into the technological route. And, as mentioned above, this contributes to a decrease in responsivity. The number of thermal operations can be reduced with the simultaneous diffusion of boron to the front and back sides of the substrate. This will make it possible to simultaneously form surface areas of the limitation of p^+-type leakage channels on the front side, and to form an ohmic contact on the back side of the plate. However, in this case, there is a need to form a masking coating on the surface of the p^+-regions of the front side.

The SiO_2 masking layer can be formed by any other method other than thermal oxidation. In particular, by pyrolysis of alkyloxylans, hydrolysis of silicon halogens or monosilane, as well as by vacuum cathodic deposition. However, this is complicated by the need to maintain the thickness of the anti-reflective silicon oxide, which corresponds to the minimum reflection. Here, it is necessary to pre-etch SiO_2 (partially or completely).

Another option is to apply another type of dielectric, for example Al_2O_3. In this way, a two-layer structure with a lower reflection coefficient (in the case of applying an optimized thickness) can be formed on the surface of the REs than on the SiO_2 itself, and on the surface of the

p^+-regions, aluminum oxide will perform a masking function.

The above mentioned requires additional research.

References

1. Kukurudziak, M. S. Influence of Surface Resistance of Silicon p-i-n Photodiodes n^+-Layer on their Electrical Parameters. *Physics and chemistry of solid state*, 2022, vol. 23, no 4, pp. 756-763. DOI: 10.15330/pcss.23.4.756-763.

2. Sun, K., Gao, J., Costanzo, R., Tzu, T.-C., Bowers, S. M., Beling, A. Germanium Photodiode Arrays on Silicon-On-Insulator with On-Chip Bias Circuit. *IEEE Photonics Technology Letters*, Aug. 15 2021, vol. 33, no. 16, pp. 832-835. DOI: 10.1109/LPT.2021.3064505.

3. Liu, L., Wu, Z., Qi, M., Li, Y., Zhang, M., Liao, D., Gao, P. Application of Adaptive Optics in Ophthalmology. *Photonics*, 2022, vol. 9, no. 5, article id: 288. DOI: 10.3390/photonics9050288.

4. Rank, E. A., Agneter, A., Schmoll, T., Leitgeb, R. A., Drexler, W. Miniaturizing optical coherence tomography. *Translational Biophotonics*, 2022, vol. 4, no. 1-2, article id: e202100007. DOI: 10.1002/tbio.202100007.

5. Demir-Yilmaz, I., Guiraud, P., Formosa-Dague, C. The contribution of Atomic Force Microscopy (AFM) in microalgae studies: A review. *Algal Research*, 2021, vol. 60, article id: 102506. DOI: 10.1016/j.algal.2021.102506.

6. *Pasport FD 342M* [Data Sheet PD 342M]. Available at: https://orion-ir.ru/upload/iblock/ccb/ccb64e81f708470ee2c2e4699b9679e2.pdf (accessed 12.10.2022).

7. *Data Sheet YAG-555-4*. Available at: https://www.excelitas.com/product/yag-555-4-series-quadrant-photodiodes-si-pin-141-mm (accessed 12.10.2022).

8. *Pasport FD 15M-01* [Data Sheet PD 15M-01]. Available at: http://www.ckb-rhythm.narod.ru/FD_SPIN/ufd15m-01.htm (accessed 12.10.2022).

9. *Data Sheet QP154-Q*. Available at: https://www.first-sensor.com/cms/upload/datasheets/QP154-Q_HVSD_5000023.pdf (accessed 12.10.2022).

10. Demidov, S. S., Klimanov, E. A., Nuri, M. A. Kremnevyy koordinatniy fotodiod s uluchshennymi parametrami [The coordinate silicon photodiode with improved parameters]. *Prykladnaya fyzyka – Applied Physics*, 2014, no. 4, pp. 73-75. [in Russian].

11. Moskalenko, V. V., Moskalenko, A. S., Korobov, A. H., Zarets'kyy, M. O., & Semashko, V. A. Model' ta alhorytm navchannya systemy detek-tuvannya malorozmirnykh ob"yektiv dlya malohaba-rytnykh bezpilotnykh lital'nykh aparativ [A model and learning algorithm of small-sized object detection system for compact drones]. *Radioelektronni i komp'uterni sistemi – Radioelectronic and computer systems*, 2018, no. 4, pp. 41-52. DOI: 10.32620/reks.2018.4.04. [in Ukrainian].

12. *GOST 1772-88. Priyemniki izlucheniya. Poluprovodnikovyye fotoelektricheskiye i fotopriyemnyye ustroystva. Metody izmereniya fotoelektricheskikh parametrov i opredeleniye kharakteristik* [GOST 1772-88. Radiation detectors. Semiconductor photovoltaic devices and photodetector preamplifier modules. Methods of measuring photoelectric parameters and determination of characteristics: Effective from 1988-01- 07. Moscow, Standards Publishing House, 1988. 158 p. (State Standard of the USSR) [in Russian].

13. Sun, S. C., Plummer, J. D. Electron Mobility in Inversion and Accumulation Layers on Thermally Oxidized Silicon Surfaces. *IEEE Journal of Solid-State Circuits*, Aug. 1980, vol. 15, no. 4, pp. 562-573. DOI: 10.1109/JSSC.1980.1051439.

14. Nikoghosyan, H. S., Nikoghosyan G., Demirchian, H. G. Optical resonance in the inversion n−channel of a silicon MOS structure. *Physica B: Condensed Matter*, 2022, vol. 639, article no. 414018. DOI: 10.1016/j.physb.2022.414018.

15. Scinner, S. M. Improve device reliability whith physics-of-failure techniques. *Electronsc Design*, 1965, vol. 13, pp. 70-75.

16. Kukurudziak, M. S. 1064 nm wavelength p-i-n photodiode with low influence of periphery on dark currents. *Journal of nano- and electronic physics*, 2022, vol. 14, no 1, article no. 01023. DOI: 10.21272/jnep.14(1).01023.

17. Atalla, M. M., Tannenbaum, E., Scheibner, E. J. Stabilization of Silicon Surfaces by Thermally Grown Oxides. *Bell System Technical Journal*, May 1959, vol. 38, iss. 3, pp. 749-783. DOI: 10.1002/j.1538-7305.1959.tb03907.x.

18. Kukurudziak, M. S., Maistruk, E. V. Features of Diffusion Doping and Boron Gettering of Silicon pin Photodiodes. *IEEE 3rd KhPI Week on Advanced Technology (KhPIWeek)*, 2022, pp. 1-6. DOI: 10.1109/KhPIWeek57572.2022.9916420.

19. Jeyaselvan, V., Selvaraja, S. K. Lateral Dopant Diffusion Length Measurements Using Silicon Microring Resonators. *IEEE Photonics Technology Letters*, 2018, vol. 30, iss. 24, pp. 2163-2166. DOI: 10.1109/LPT.2018.2879574.

20. Hamasaki, H., Suzuki, J., Shimada, T. F. Lateral effect of oxidation enhanced diffusion in silicon. *1981 International Electron Devices Meeting*, Washington, DC, USA, 1981, pp. 542-545. DOI: 10.1109/IEDM.1981.190140.

21. Seshan, K., Schepis, D. *Handbook of Thin Film Deposition*. William Andrew, Publ. 2018. 470 p.

ISSN 1814-4225 (print)
ISSN 2663-2012 (online)

22. Klemmt, A., Lange, J., Weigert, G., Lehmann, F., Seyfert, J. A multistage mathematical programming based scheduling approach for the photolithography area in semiconductor manufacturing. *Proceedings of the 2010 Winter Simulation Conference*, Baltimore, MD, USA, IEEE, 2010, pp. 2474-2485. DOI: 10.1109/WSC.2010.5678943.

23. Kukurudziak, M. S. Formation of Dislocations During Phosphorus Doping in the Technology of Silicon p-i-n Photodiodes and their Influence on Dark Currents. *Journal of nano- and electronic physics*, 2022, vol. 14, no 4, article no. 04015. DOI: 10.21272/jnep.14(4).04015.

Надійшла до редакції 29.12.2022, розглянута на редколегії 20.02.2023

КРЕМНІЄВИЙ ЧОТИРИЕЛЕМЕНТНИЙ P-I-N ФОТОДІОД ІЗ ПОКРАЩЕНИМИ ХАРАКТЕРИСТИКАМИ

Микола Кукурудзяк

У статті наведено результати розробки кремнієвих координатних p-i-n фотодіодів (ФД) з покращеними параметрами. Досліджено технологічні можливості зменшення зазорів між фоточутливими площадками багатоелементних ФД. Змодельовано ФД зі зменшеними зазорами, виготовлено зразки згідно моделей, досліджено параметри отриманих ФД та вплив різних технологічних факторів на їх значення. Під час досліджень встановлено, що фактором, який обмежує можливість зменшення зазорів є опір ізоляції між фоточутливими елементами (ФЧЕ). Зменшення опору ізоляції між елементами ФД було наслідком утворення інверсійних каналів витоку на межі $Si\text{-}SiO_2$, що є характерним для високоомного кремнію p-типу, провідність яких зростала при зменшенні ширини зазорів. Для підвищення опору зазорів між площадками та мінімізації впливу інверсійних шарів вирішено утворити між ФЧЕ області обмеження каналів витоку – сильно леговані області, ізотипні з матеріалом підкладки (p^+-типу). Вони запобігатимуть руху носіїв струму, які генеруються в інверсійних шарах на поверхні підкладки. Виготовлено чотири-елементі p-i-n фотодіоди із зазорами між площадками 31 мкм. Запропонований ФД не значно поступається параметрами аналогам, але є зразком із найменшими зазорами між ФЧЕ серед фотодіодів такого ж типу та розміру на ринку. Покращення опору ізоляції між ФЧЕ дозволило знизити рівень темнового струму ФД в два рази порівняно із серійними виробами, при незначному зниженні фоточутливості внаслідок введення в технологічний маршрут додаткових термічних операцій. Зокрема, густина темнового струму ФЧЕ експериментальних ФД складала 40-80 нА/см^2, порівняно з 80-250 нА/см^2 для серійних зразків. Імпульсна струмова монохроматична чутливість на довжині хвилі 1064 нм для експериментальних зразків складала 0,41-0,44 А/Вт, а для серійних – 0,45-0,48 А/Вт

Ключові слова: фотодіод; фоточутливі елементи; фоточутливість; темновий струм; опір ізоляції.

Кукурудзяк Микола Степанович – інженер-технолог 1кат., АТ «Центральне конструкторське бюро Ритм»; аспірант кафедри електроніки і енергетики ІФТКН Чернівецького національного університету імені Юрія Федьковича за спеціальністю «Електроніка», Чернівці, Україна.

Mykola Kukurudziak – technologist engineer 1 cat. Rhythm Optoelectronics Shareholding Company; PhD student in the specialty "Electronics" of Electronics and Power Engineering Department, Yuriy Fedkovych Chernivtsi National University, Chernivtsi, Ukraine,
e-mail: mykola.kukurudzyak@gmail.com, ORCID: 0000-0002-0059-1387, Scopus Author ID: 57454991100.